Spatial and Temporal Variability of Rotational, Focal and Irregular Activity: Practical Implications for Mapping of Atrial Fibrillation

Michael Pope[1], Pawel Kuklik[2], Andre Briosa e Gala[1], Milena Leo[1], Michael Mahmoudi[3], John Paisey[4], and Tim Betts[5]

[1]Oxford University Hospitals NHS Foundation Trust
[2]Asklepios Kliniken Hamburg GmbH
[3]University of Southampton Faculty of Medicine
[4]University Hospital Southampton
[5]Oxford University Hospitals NHS trust

March 22, 2021

Abstract

Background Charge density mapping of atrial fibrillation (AF) reveals dynamic patterns of localised rotational activation (LRA), irregular activation (LIA) and focal firing (FF). Their spatial stability, conduction characteristics and the optimal duration of mapping required to reveal these phenomena and has not been explored. Methods Bi-atrial mapping of AF propagation was undertaken and variability of activation patterns quantified up to a duration of 30-seconds(s). The frequency of each pattern was quantified at each vertex of the chamber over 2 separate 30s recordings prior to ablation and R2 calculated to quantify spatial stability. Regions with the highest frequency were identified at increasing time durations and compared to the result over 30s using Cohen's kappa. Properties of regions with the most stable patterns were assessed during sinus rhythm and extrastimulus pacing. Results In twenty-one patients, 62 paired LA and RA maps were obtained. LIA was highly spatially stable with R2 between maps of 0.83(0.71-0.88) compared to 0.39(0.24-0.57) and 0.64(0.54-0.73) for LRA and FF, respectively. LIA was also most temporally stable with a kappa of >0.8 reached by 12s. LRA showed greatest variability with kappa>0.8 only after 22s. Regions of LIA were of normal voltage amplitude (1.09mv) but showed increased conduction heterogeneity during extrastimulus pacing (p=0.0480). Conclusion Irregular activation patterns characterised by changing wavefront direction are temporally and spatially stable in contrast with rotational patterns that are transient with least spatial stability. Focal activation appears of intermediate stability. Regions of LIA show increased heterogeneity following extrastimulus pacing and may represent fixed anatomical substrate.

Spatial and Temporal Variability of Rotational, Focal and Irregular Activity: Practical Implications for Mapping of Atrial Fibrillation

First author: Pope MTB.

Short title: Spatiotemporal variability of propagation during atrial fibrillation.

Authors: Michael TB Pope BM BSc[1,2], Pawel Kuklik PhD[3], Andre Briosa e Gala MD[1], Milena Leo MD[1], Michael Mahmoudi MBBS PhD[2], John Paisey DM[2], Timothy R Betts MD[1,4]

Affiliations and contacts:

1. Oxford University Hospitals NHS Foundation Trust
2. University of Southampton, UK
3. Department of Cardiology, Asklepios Clinic St. Georg, Hamburg, Germany

4. University of Oxford Biomedical Research Centre, UK

Corresponding author: Michael Pope, Research Fellow Office, Department of Cardiology, John Radcliffe Hospital, Headley Way, Oxford, OX3 9DU.

Michael.pope@ouh.nhs.uk ORCID ID: https://orcid.org/0000-0002-4166-3746

PK: p.kuklik@asklepios.com

AG: Andre.gala@ouh.nhs.uk

ML: milena.leo@ouh.nhs.uk

MM: m.mahmoudi@soton.ac.uk

JP: john.paisey@uhs.nhs.uk

TB: Tim.betts@ouh.nhs.uk ORCID ID: 0000-0001-9063-9905

Abbreviations

ACT: Activated clotting time

AF: Atrial fibrillation

CHI: Conduction Heterogeneity Index

FF: Focal firing

MAT: Median Activation Time

LA: Left atrium

LIA: Localised irregular activation

LRA: Localised rotational activation

persAF: Persistent atrial fibrillation

RA: Right atrium

Abstract

Background

Charge density mapping of atrial fibrillation (AF) reveals dynamic patterns of localised rotational activation (LRA), irregular activation (LIA) and focal firing (FF). Their spatial stability, conduction characteristics and the optimal duration of mapping required to reveal these phenomena and has not been explored.

Methods

Bi-atrial mapping of AF propagation was undertaken and variability of activation patterns quantified up to a duration of 30-seconds(s). The frequency of each pattern was quantified at each vertex of the chamber over 2 separate 30s recordings prior to ablation and R^2 calculated to quantify spatial stability. Regions with the highest frequency were identified at increasing time durations and compared to the result over 30s using Cohen's kappa. Properties of regions with the most stable patterns were assessed during sinus rhythm and extrastimulus pacing.

Results

In twenty-one patients, 62 paired LA and RA maps were obtained. LIA was highly spatially stable with R^2 between maps of 0.83(0.71-0.88) compared to 0.39(0.24-0.57) and 0.64(0.54-0.73) for LRA and FF, respectively. LIA was also most temporally stable with a kappa of >0.8 reached by 12s. LRA showed greatest

variability with kappa>0.8 only after 22s. Regions of LIA were of normal voltage amplitude (1.09mv) but showed increased conduction heterogeneity during extrastimulus pacing (p=0.0480).

Conclusion

Irregular activation patterns characterised by changing wavefront direction are temporally and spatially stable in contrast with rotational patterns that are transient with least spatial stability. Focal activation appears of intermediate stability. Regions of LIA show increased heterogeneity following extrastimulus pacing and may represent fixed anatomical substrate.

Keywords:

Atrial fibrillation, AcQMap, Charge Density Mapping, Spatiotemporal stability, Localised irregular activation

Condensed abstract

Atrial fibrillation propagation patterns including localised irregular activation patterns (LIA), rotational activation patterns (LRA) and focal firing (FF) can be identified using non-contact mapping. LIA is characterised by repeated localised wavefront directional change and demonstrates high spatiotemporal stability alongside regions with high frequency FF. In contrast, LRA is transient and inconsistent. We therefore speculate that regions of high frequency LIA may best reflect atrial structural aberrations whilst LRA is a functional reflection of wavefront dynamics.

Introduction

The limited efficacy of pulmonary vein isolation for the ablation of persistent atrial fibrillation (persAF) has resulted in concerted efforts to identify non-pulmonary vein mechanisms responsible for AF maintenance. This has led to the development of techniques to facilitate mapping of the underlying atrial electrophysiology with the aim of revealing fibrillatory mechanisms and guiding targeted ablation.(1-6)

Non-contact charge-density mapping allows visualisation of whole chamber activation. Wavefront patterns are scrutinised in real time at every vertex of the chamber surface (approximately 3,500) by in an inbuilt application (AcQTrack, Acutus Medical). Non-planar, complex localised patterns of propagation are identified and characterised as localised rotational activation (LRA), localised irregular activation (LIA) and focal firing (FF)(see figure 1).(7) To be classed as LRA, a smooth depolarisation wavefront has to rotate 360 degrees around a central point. LIA is characterised by a difference in angle between conduction that enters and leaves a confined region exceeding a threshold of 90 degrees (and not meeting the criteria for LRA above). In contrast, FF is defined as activation of a primary vertex that precedes adjoining neighbours and extends centrifugally from this primary vertex.

A catheter ablation approach aimed at targeting these zones has been evaluated in one prospective observational study,(6) but little work has been done exploring the spatial and temporal stability of these electrophysiological phenomena and the properties of these regions in sinus rhythm, knowledge of which is crucial in developing an optimal approach. We sought to investigate the spatial stability between 2 separate 30-second recordings of left and right atrial AF propagation and the effects of increasing duration of AF recording length on the degree of variability in mechanisms observed during simultaneous bi-atrial mapping of atrial fibrillation. Properties of atrial regions with the most stable patterns were explored using long and short cycle length pacing and electroanatomic voltage mapping in sinus rhythm.

Methods

Patient selection

Patients between the ages 18-80 undergoing first time catheter ablation for either paroxysmal (n=5) or persistent (n=17) AF were recruited following appropriate ethical approval (REC reference 18/SC/0409, clinicaltrials.gov NCT03812601). Exclusion criteria included prior cardiac surgery, congenital cardiac abnormalities and severe valvular heart disease.

Electrophysiological mapping and ablation

Procedures were carried out under general anaesthetic. With the exception of amiodarone, antiarrhythmic drugs were stopped a minimum of five days prior to the procedure. Venous access was obtained via bilateral femoral vein puncture under direct ultrasound guidance. Heparin boluses were administered prior to transseptal puncture followed by continuous heparin infusion to maintain an ACT >350s. A decapolar catheter (Inquiry, Abbott Medical) was inserted into the coronary sinus through an AcQRef (Acutus Medical) sheath which includes a distal electrode used as a unipolar reference. The first AcQMap catheter was advanced over a 0.032 guide wire into the RA via an AcQGuide (Acutus Medical) sheath and ultrasound used to reconstruct the right atrial chamber anatomy as previously described.[7] The ablation catheter (Tacticath, Abbott Medical) was advanced via an Agilis sheath into the left atrium across the single transseptal puncture site. The second AcQGuide sheath was then exchanged for the transseptal access sheath over the guide wire and a second AcQMap catheter advanced into the LA (see figure 2). The LA anatomy was then generated with ultrasound. A circular mapping catheter (Inquiry Optima or Advisor Variable Loop, Abbott Medical) was used to undertake electroanatomic voltage mapping and guide pulmonary vein isolation.

In a subset of 9 patients, activation maps were obtained using Supermap during pacing from up to three atrial sites (left atrial appendage, high right atrium and proximal coronary sinus) with direct cardioversion used to restore sinus rhythm where necessary. Pacing consisted of a 4-beat drive train at 800ms cycle length followed by a single extrastimulus with coupling interval 20ms above the effective refractory period and was mapped using the AcQMap Supermap algorithm. Additional details are provided in the supplementary methods.

In patients attending the procedure in sinus rhythm AF was induced using burst atrial pacing, otherwise all AF recordings were obtained prior to DCCV. Once AF was established, recordings of 2 minutes duration were generated and time alignment between systems facilitated using a below threshold pacing stimulus from the coronary sinus catheter of 4 beats at 1000, 800 and 600ms intervals and 12 second rest period. Pulmonary vein isolation was performed using contact force guided radiofrequency ablation using 40-50 Watts (Tacticath ablation catheter, Abbott Medical). Simultaneous biatrial AF mapping was repeated following completion of PVI. Additional ablation and AF mapping was undertaken at the discretion of the operator.

Propagation Map Calculation and Data Export

Raw AcQMap electrode biopotential signals were visually inspected to identify outlying or corrupted signals, which were then manually excluded. A low pass filter at 100Hz as well as a 50Hz notch filter and smoothing algorithm were applied followed by selection of a QRS-T wave template for subtraction. Three consecutive 10-second mapping segments were created for simultaneous timepoints in both the left and right atria, confirmed relative to the coronary sinus low amplitude pacing spike. This process was repeated to create two 30-second AF maps following splicing together of each 10s segment. Propagation maps were calculated using the default timing method (based on -dv/dt of dipole signals), window width (for isochronal colour bars) of 80ms and time threshold of 70ms (representing presumed minimum refractoriness). AcQTrack propagation patterns were calculated for each segment and data exported for offline analysis.

Propagation Pattern Quantification

Complex propagation patterns described above (LIA, LRA and FF) were identified using the AcQTrack (Acutus Medical) system during AF to ensure objective classification of activation patterns, as outlined in the supplementary methods. Representative examples of these patterns are seen in figure 1 and supplementary videos 1-3. Every wavefront is scrutinised at each vertex of the anatomy. Planar wavefronts are discarded, whilst if the parameters for LIA, LRA and FF are met within a discreet zone ($300mm^2$ for LRA and $200mm^2$ for LIA) the vertices within this zone are highlighted and recorded by the system.

These data were exported and analysed using a custom designed programme to allow quantification. The process is outlined in figure 3 and supplementary figure S3. Initially, all AcQTrack data is exported to create a static map quantifying every pattern occurrence at each vertex of the chamber anatomy (approximately

4

3500 per chamber) for the entire recording duration (3A). Each single occurrence is signified by a disc that occurs in a specific region for the duration that pattern is present (3B). The number of these unique "discs" equates to the number of occurrences of the specified propagation pattern. When taken over the duration of the recording, the proportion of time in which these discs are detected on the chamber surface represents the time parameter. Similarly, the proportion of the chamber in which an occurrence is detected represents the surface area affected.

A cut off threshold is then applied to exclude outlying data and identify the localised region with the most repetitive pattern occurrences. The number of occurrences in each region and the proportion of time that they are present are known. These factors are used to determine the optimum threshold as outlined in figure 4. The initial static map displays all occurrences with no cut off applied (zero on the x axis i.e. every occurrence is counted). The percentage of the recording time with the relevant pattern is shown on the Y axis. As the cut off is increased along the X axis (i.e. only regions with increasing numbers of occurrences are included), the proportion of time these are present decreases. A threshold is applied relative to the total time pattern occurrences are present. In the example in figure 4, (for LIA) with no cut off, LIA was present for 85% of the mapping duration. Increases in the threshold resulted in a reduction in the percentage of time that LIA was present. A 10% threshold excludes LIA to the point at which only regions with LIA present for 75% of the recording duration are counted, which corresponds to more than 6 occurrences over the duration of the recording. Similarly, a threshold that corresponds to a 30% relative reduction from the initial maximum duration identifies the region with only the highest number of occurrences. Where discs representing a detection are overlapping at any time point (potentially representing a meandering central pivot or rotation point) these are counted as a single pattern detection. Once a cut off is applied, only occurrences with the geometric centre of the "disc" within the specified zone are included for quantification and any occurrence detected within 5ms of a preceding occurrence in the same location is excluded to avoid double counting.

Spatial stability

Spatial stability was assessed by correlating the frequency of propagation patterns (LIA, LRA and FF) at each vertex of the chamber anatomy over 2 separate 30s recordings taken at baseline prior to any ablation. The value for the number of pattern occurrences were plotted for each vertex of the anatomy for each recording. A linear best fit line was plotted, and R^2 calculated to assess the strength of the linear correlation between the two mapping segments. Stability of regions with the most repetitive patterns identified using the 30% threshold value for each 30s map were compared using Cohen's kappa statistic.

Temporal Stability/Optimal Mapping Duration

The region with the highest frequency of each propagation pattern may be considered as reflecting an optimum target for ablation. This was identified using the 30% cut off to identify the relevant zone on maps of increasing duration up to 30 seconds. Each vertex of the anatomy contained within and outside this region (at 30% cut off) was used to calculate the kappa statistic to quantify the consistency between these zones against the zone identified during a full 30 second segment. Kappa values were calculated and plotted at both 1-second and 5-second increments with a value of 0.8 considered excellent consistency compared to the result obtained at 30-seconds. The duration at which a kappa value of 0.8 was reached was extracted for each map and used for comparisons.

In a subset of 15 patients, additional analyses were undertaken using alternative methods to confirm that the results obtained were consistent between methods used. LIA, LRA, and FF were quantified for occurrence frequency, percentage time present and percentage of the chamber surface area affected (for FF only frequency was assessed) at increasing durations, also in 1-second increments up to 30-seconds. At each incremental recording duration, the percentage change in each variable was calculated. For occurrence frequency the results for every possible combination of maps of increasing duration within the 30s recording were compared (e.g. the frequency of a pattern was measured over 5-seconds and compared with all possible maps of 5-second duration within the full 30-second recording). For occurrence time and surface area a 5s moving average at

5

1s increments was calculated. Heatmaps were created for each pattern allowing a visual representation of the effect of duration on variability.

Electroanatomic Voltage mapping and Conduction Heterogeneity

Left and right atrial geometries created using Ensite Precision were exported and fused with the AcQMap anatomies using fiducial points and a nearest neighbour approach to assign bipolar voltage amplitude to each site on the AcQMap chamber enabling comparison between sites according to identified activation patterns.

Activation time maps obtained using Supermap were exported and analysed offline. The local activation time difference (LAT) for a 5mm radius from every vertex of the anatomy was calculated for each map and the largest value taken for each point to generate a histogram. The median LAT difference (MAT) and the conduction heterogeneity index (CHI) (95th percentile - 5^{th}percentile/median) was calculated within regions shown to demonstrate stable high frequency activation patterns during AF as described previously(8) and the effect of extrastimulus pacing on the CHI calculated in these regions compared to the remainder of the chamber.

Statistics

Continuous variables are expressed as mean $\pm$ standard deviation or median and interquartile range depending on distribution. Between group comparisons were performed using independent samples t-test or Wilcoxon rank sum test depending on distribution as assessed using the Kolmogorov-Smirnov test. A two-sided p value of <0.05 was considered significant. Statistical analysis was performed using SPSS (IBM v25) or Matlab (R2019a, MathWorks) and figures created using Matlab.

Results

Patient Characteristics and Map Segments Obtained

The characteristics of all patients recruited to the study are outlined in table 1. One patient (patient 9) was excluded from analysis as only organised atrial tachycardia could be induced when attending for the procedure. In all but one patient (patient 12), two 30-second maps of AF were obtained at baseline. Patient 12 had varying QRS morphology as a result of left bundle branch block and only one 30s segment could be obtained with sufficient quality of QRS-T wave subtraction to allow analysis. Maps following pulmonary vein isolation were obtained in 12 patients and a further 8 recordings were obtained following non-pulmonary vein ablation providing a total of 62 simultaneous AF recordings in the left and right atrium. Mapping duration and temporal variability analysis was performed on all maps obtained (a total of 124 maps including both chambers). Spatial variability analysis was performed by comparing the two 30s maps obtained at baseline in the 20 patients.

Spatial Variability

LIA demonstrated the greatest spatial stability with R^2 of 0.83(0.71-0.88) across all maps analysed. This was consistent across both chambers with values of 0.81(0.75-0.88) and 0.84(0.61-0.88) in the LA and RA respectively. Median R^2 for LRA and FF were 0.39(0.24-0.57) and 0.64(0.54-0.73) respectively. Multiple low frequency focal firings were seen widely distributed across the atrial surface (see figure 5). For high frequency FF, defined as occurring [?]10 times over the 30s, R^2 was 0.83(0.68-0.85). Detailed results are outlined in table 2.

Stability of regions across both maps with the highest frequency patterns identified at 30% cut off was also greatest for LIA in both the LA and RA. Cohen kappa statistic for LIA in the LA and RA respectively was 0.75 (0.64-0.78) and 0.75 (0.58-0.79). Full kappa statistic results for all patients are outlined in table 3.

The anatomical regions with maximal LIA were the anterior and posterior LA (in 46% and 27% of maps respectively) and the lateral and septal RA (in 46% and 32% respectively). LRA showed similar distribution with the zone of highest LRA frequency in the posterior LA in 41% and the anterior LA in 34%. In the RA, the lateral wall was the most common site (in 37%) followed by the septum and posterior walls (each

6

in 24%). A similar distribution was observed for FF, most commonly involving the anterior and posterior LA (in 34% and 29% respectively), followed by the LA septum (20%). In the RA, the highest frequency of FF was seen in the septum in 59% and the lateral wall in 22%.

Mapping duration results

Figure 6 demonstrates the effect of increasing map duration on kappa statistic values for LIA, LRA and FF respectively compared to maps of 30 seconds. Analysis was conducted on all 124 recordings (62 in the LA and 62 in the RA) obtained. LIA showed the highest kappa value at all time periods with a value of 0.66 (0.57-0.70) at 5s, rising to 0.93 (0.91-0.95) at 25s. LRA demonstrated the lowest value of 0.32 (0.17-0.43) at 5s, with a maximum of 0.85 (0.79-0.91) at 25s. A kappa value of 0.8 can be considered excellent correlation. Figure 6D shows kappa values at 1-second increments for LIA, LRA and FF. A value for 0.8 was reached by 12-seconds (IQR 6) for LIA compared to 19-seconds (IQR 7) for FF (p<0.0005) and 22-seconds (IQR 8) for LRA (p<0.0005).

The duration of mapping required to achieve a kappa value of 0.8 was compared between the left and right atria, in patients with paroxysmal and persistent AF, before and after pulmonary vein isolation and in patients on or off amiodarone. There was no difference for any parameter between the left and right atria. In patients with persistent AF, LIA stabilised earlier than in patients with paroxysmal AF (11+-6 versus 15+-4, difference 4-seconds, 95% confidence interval 0.6-5.6, p=0.004). There was no difference between any groups for stability of LRA. The frequency of focal firing stabilised after 17.2+-5.6 seconds following pulmonary vein isolation compared to 19.1+-3.7 seconds prior to pulmonary vein isolation, a difference of 1.9-seconds (95% CI 0.3-3.6, p=0.023). Full results for all comparisons are in supplementary figures S6 and S7 and tables S1-S3.

Heatmaps for the subset of 15 patients are shown in supplementary figure S8. When measured as either a frequency, proportion of time the propagation pattern was present or a proportion of the atrial surface area that patterns occurred, variability in LIA fell rapidly, followed by FF and LRA. A significant degree of variability in LRA patterns was observed, particularly when measured as a proportion of the atrial surface affected up to durations of 20-25s.

Voltage and Conduction Properties

The median distance between merged chamber surfaces was 6.0mm (IQR 3.4-10.7). The voltage in regions of high frequency LIA was 1.09mv (IQR 0.55-1.94) compared to 1.07mv (IQR 0.51-1.94) in the remainder of the chamber (p=0.9936).

A total of 53 paired maps at long and short cycle length were obtained for the LA and RA in a subset of 9 patients (in 1 participant only 2 sites were obtained due to AF induction). The MAT across all maps obtained in regions with high frequency LIA was 7.5ms (IQR 6.6-8.9) compared to 6.0ms (IQR 5.2-7.7) in the remainder of the chamber, a statistically significant difference of 1.5ms, p<0.0005. Extrastimulus pacing resulted in a significant increase in CHI in regions of high frequency LIA from 3.3 (IQR 2.3-4.4) to 4.0 (IQR 3.1-5.4) (p=0.0480), but no increase in the remainder of the chamber (p=0.4636) as shown in figure S9.

Discussion

This study demonstrates that regions with LIA patterns show high spatiotemporal stability. In contrast rotational activation patterns, closest to the 'rotors' identified using other mapping techniques, show the least spatiotemporal stability. Regions of high frequency FF are relatively more stable whereas infrequent FF is not. Mapping durations of 20-25s are required to identify all temporally variable propagation patterns although shorter durations will identify the most stable LIA and FF. Although bipolar voltage amplitude in these regions is normal, they demonstrate an increase in conduction heterogeneity during short coupled extrastimulus pacing.

The aim of technologies designed to facilitate electrophysiological mapping and ablation of AF mechanisms is to identify repetitive patterns within a characteristically disorganised rhythm. The total duration analysed

has a significant impact on how a repetitive pattern is defined and there have been limited efforts previously to determine the optimum duration required. Studies often do not report the duration of AF mapped but may report that patterns identified are stable over several minutes and separate recordings.(1, 9, 10) Other studies have used recording durations of between 10 seconds and 5 minutes.(3, 5, 11) Of note a retrospective analysis where 5 minute initial recordings were used found that 89% of the mechanistic sites identified were also seen when 30s recording durations were analysed.(12) However, shorter durations than this were not assessed. It may be revealing that when only 10s recording durations have been chosen, in the study by Child et al using a technique of basket contact mapping and phase singularity analysis, spatially stable patterns were not identified.(3) Rotational activation patterns demonstrate the least stability between and during recordings, with 10s of mapping showing only very moderate correlation with the results obtained from 30s mapping (kappa 0.55) and a variability in rotational activation pattern frequency of approximately 20% at a duration of 10s. Of note, of course, is that durations beyond 30s were not assessed and it may be that accuracy improves yet further if longer analyses are performed.

Traditional electrophysiological assessment has involved mapping of either the endocardial or epicardial surfaces. There is increasing recognition that the remodelling involved in the development and progression of AF is a three-dimensional process resulting in activation time differences between atrial surfaces.(13, 14) In this context, epicardial propagation that results in local breakthrough conduction will manifest as a focal activation pattern on the endocardial surface. The sites of epicardial breakthrough are likely to either be randomly distributed, if arising from chaotic 3-dimensional propagation, or recur at specific sites where the remodelling process promotes breakthrough to the endocardial surface. Sporadic focal activations and random breakthroughs are likely to display minimal consistency across recordings whilst high frequency activations or sites of recurrent breakthrough are likely to be consistent. This was supported by the finding of much greater correlation at high frequency sites (R^2 value 0.83, IQR 0.17) than when all activations are considered (R^2 0.64, IQR 0.19). However, distinguishing between a site of recurrent breakthrough and true focal activation is not possible using the mapping methods described here. There similarly appears to be earlier stabilisation of focal firing variability following pulmonary vein isolation. This suggests a greater degree of stability in non-pulmonary vein sites of focal activation.

The spatial consistency of LIA detection between separate recordings is illustrated in figure 5. Bipolar voltage amplitude in these regions is normal, which suggests that the activation properties observed are not the result of dense fibrosis. However, bipolar voltage amplitude is a relatively crude tool and is highly dependent on both rate and vector of activation(15). Studies using late gadolinium enhanced magnetic resonance imaging reveal patchy areas of fibrosis out of keeping with the burden seen on voltage mapping studies(16, 17) suggesting the existence of interstitial fibrosis that is not revealed by measuring bipolar voltage amplitude. The MAT during pacing within LIA zones was longer, suggestive of slower conduction velocity, and short coupled extrastimulus pacing resulted in an increase in CHI in these regions that was not observed in the remainder of the chamber. Although these sites may represent anatomically normal regions of changing fibre orientation resulting in anisotropic conduction, they may represent disrupted conduction caused by underlying atrial interstitial fibrosis resulting in fibre disarray and rate dependent conduction abnormalities that manifest as local irregular activation patterns during AF. In a study by Walters et al. using surgically placed epicardial plaques in patients with longstanding persistent AF, disorganised activation was frequently observed, which did not satisfy criteria for either rotors or focal activations but was stable over multiple recordings of 10s duration taken over a period of 10 minutes(18). This disorganised activation may represent similar propagation patterns to the irregular activation observed using charge density mapping, which was similarly stable even at short mapping durations. Walters also reported that rotors were frequently transient, in keeping with the results outlined here.

Both the non-hierarchical multiple-wavelet hypothesis and the competing "mother-rotor", or focal driver, hypothesis describe a process of wave-break in the formation of fibrillatory wavefronts involved in maintenance of cardiac fibrillation.(19, 20) Tissue homogeneity is thought to play a significant role in the susceptibility to fibrillation(21) with regions of structural inhomogeneity likely responsible for the wave-break that results in

8

fibrillatory conduction.(22) The anatomical regions demonstrating stable LIA patterns identified in this study may therefore reflect sites of structural heterogeneity responsible for wave-break, and therefore play an important role in AF maintenance.

Importantly, this study was not designed to assess ablation strategy or effectiveness and is not able to determine the impact of the phenomena identified on AF maintenance. This requires further detailed work. However, an understanding of the transient properties of rotational activity and low frequency focal activations observed in short mapping segments is crucial to designing ablation strategies that can be tested in clinical trials and suggests they are unlikely to occur as a result of anatomical substrate, such as scar or myofibre architecture. Targeting a fixed therapy to transient, migratory activation patterns is likely to be ineffective.

Conclusion

Charge density mapping facilitates identification of complex patterns of wavefront propagation during atrial fibrillation. Although irregular activation patterns characterised by changing wavefront direction, and high frequency focal firing are spatially stable, rotational activations are transient and meandering, with low spatial stability. The duration of mapping recording used significantly impacts the results obtained. A minimum duration of 20s is required to identify regions of repetitive but transient rotational activation whilst shorter segments will accurately reveal regions with high frequency irregular and focal activation. These stable regions of irregular activation may best reflect underlying atrial structural abnormalities and represent important sites for catheter ablation approaches.

Funding sources

Disclosures

MP has received honoraria and support for conference attendance from Acutus Medical.

PK provides consultancy services to Acutus Medical.

TB has received honoraria from Acutus Medical and is a member of their Medical Advisory Board.

References

1. Narayan SM, Krummen DE, Shivkumar K, Clopton P, Rappel WJ, Miller JM. Treatment of atrial fibrillation by the ablation of localized sources: CONFIRM (Conventional Ablation for Atrial Fibrillation With or Without Focal Impulse and Rotor Modulation) trial. J Am Coll Cardiol. 2012;60(7):628-36.

2. Haissaguerre M, Hocini M, Denis A, Shah AJ, Komatsu Y, Yamashita S, et al. Driver domains in persistent atrial fibrillation. Circulation. 2014;130(7):530-8.

3. Child N, Clayton RH, Roney CR, Laughner JI, Shuros A, Neuzil P, et al. Unraveling the Underlying Arrhythmia Mechanism in Persistent Atrial Fibrillation: Results From the STARLIGHT Study. Circ Arrhythm Electrophysiol. 2018;11(6):e005897.

4. Honarbakhsh S, Schilling RJ, Dhillon G, Ullah W, Keating E, Providencia R, et al. A Novel Mapping System for Panoramic Mapping of the Left Atrium: Application to Detect and Characterize Localized Sources Maintaining Atrial Fibrillation. JACC Clin Electrophysiol. 2018;4(1):124-34.

5. Honarbakhsh S, Hunter RJ, Ullah W, Keating E, Finlay M, Schilling RJ. Ablation in Persistent Atrial Fibrillation Using Stochastic Trajectory Analysis of Ranked Signals (STAR) Mapping Method. JACC Clin Electrophysiol. 2019;5(7):817-29.

6. Willems S, Verma A, Betts TR, Murray S, Neuzil P, Ince H, et al. Targeting Nonpulmonary Vein Sources in Persistent Atrial Fibrillation Identified by Noncontact Charge Density Mapping. Circ Arrhythm

Electrophysiol. 2019;12(7):e007233.

7. Shi R, Norman M, Chen Z, Wong T. Individualized ablation strategy guided by live simultaneous global mapping to treat persistent atrial fibrillation. Future Cardiol. 2018;14(3):237-49.

8. Roberts-Thomson KC, Stevenson IH, Kistler PM, Haqqani HM, Goldblatt JC, Sanders P, et al. Anatomically determined functional conduction delay in the posterior left atrium relationship to structural heart disease. J Am Coll Cardiol. 2008;51(8):856-62.

9. Narayan SM, Krummen DE, Rappel WJ. Clinical mapping approach to diagnose electrical rotors and focal impulse sources for human atrial fibrillation. J Cardiovasc Electrophysiol. 2012;23(5):447-54.

10. Miller JM, Kalra V, Das MK, Jain R, Garlie JB, Brewster JA, et al. Clinical Benefit of Ablating Localized Sources for Human Atrial Fibrillation: The Indiana University FIRM Registry. J Am Coll Cardiol. 2017;69(10):1247-56.

11. Honarbakhsh S, Schilling RJ, Providencia R, Keating E, Sporton S, Lowe M, et al. Automated detection of repetitive focal activations in persistent atrial fibrillation: Validation of a novel detection algorithm and application through panoramic and sequential mapping. J Cardiovasc Electrophysiol. 2019;30(1):58-66.

12. Honarbakhsh S, Schilling RJ, Finlay M, Keating E, Ullah W, Hunter RJ. STAR mapping method to identify driving sites in persistent atrial fibrillation: Application through sequential mapping. J Cardiovasc Electrophysiol. 2019.

13. Verheule S, Eckstein J, Linz D, Maesen B, Bidar E, Gharaviri A, et al. Role of endo-epicardial dissociation of electrical activity and transmural conduction in the development of persistent atrial fibrillation. Prog Biophys Mol Biol. 2014;115(2-3):173-85.

14. de Groot N, van der Does L, Yaksh A, Lanters E, Teuwen C, Knops P, et al. Direct Proof of Endo-Epicardial Asynchrony of the Atrial Wall During Atrial Fibrillation in Humans. Circ Arrhythm Electrophysiol. 2016;9(5).

15. Wong GR, Nalliah CJ, Lee G, Voskoboinik A, Prabhu S, Parameswaran R, et al. Dynamic Atrial Substrate During High-Density Mapping of Paroxysmal and Persistent AF: Implications for Substrate Ablation. JACC Clin Electrophysiol. 2019;5(11):1265-77.

16. Marrouche NF, Wilber D, Hindricks G, Jais P, Akoum N, Marchlinski F, et al. Association of atrial tissue fibrosis identified by delayed enhancement MRI and atrial fibrillation catheter ablation: the DECAAF study. JAMA. 2014;311(5):498-506.

17. Rolf S, Kircher S, Arya A, Eitel C, Sommer P, Richter S, et al. Tailored atrial substrate modification based on low-voltage areas in catheter ablation of atrial fibrillation. Circ Arrhythm Electrophysiol. 2014;7(5):825-33.

18. Walters TE, Lee G, Morris G, Spence S, Larobina M, Atkinson V, et al. Temporal Stability of Rotors and Atrial Activation Patterns in Persistent Human Atrial Fibrillation: A High-Density Epicardial Mapping Study of Prolonged Recordings. JACC Clin Electrophysiol. 2015;1(1-2):14-24.

19. Moe GK, Rheinboldt WC, Abildskov JA. A Computer Model of Atrial Fibrillation. Am Heart J. 1964;67:200-20.

20. Jalife J, Berenfeld O, Mansour M. Mother rotors and fibrillatory conduction: a mechanism of atrial fibrillation. Cardiovasc Res. 2002;54(2):204-16.

21. Weiss JN, Qu Z, Chen PS, Lin SF, Karagueuzian HS, Hayashi H, et al. The dynamics of cardiac fibrillation. Circulation. 2005;112(8):1232-40.

22. Shiroshita-Takeshita A, Brundel BJ, Nattel S. Atrial fibrillation: basic mechanisms, remodeling and triggers. J Interv Card Electrophysiol. 2005;13(3):181-93.

Tables and Figures

Table 1 Patient Characteristics

Characteristic	Distribution
AF Type	16 Persistent, 5 Paroxysmal
Sex	41% Female
Age	61 (56-66)
BMI (kg/m^2)	30 (26-33)
CHADs-VASc	1.3±1.3
Prior Anti-Arrhythmic Drugs	Sotalol: 2 (9.5%) Amiodarone: 7 (33%) Flecainide: 4 (19%)
LA Diameter (mm)	43 (38-51)
LV Ejection Fraction (%)	60 (55-60)
Time Since AF Diagnosis (Months)	48 (20-60)

Data is expressed as n(%), medians, 1st and 3rd quartiles or mean±standard deviation. Patient 9 was excluded from analysis as only atrial tachycardia could be induced. (AF: atrial fibrillation; BMI: Body mass index; LA: Left atrium; LV: left ventricle)

Table 2 R^2 values revealing the spatial stability of propagation patterns

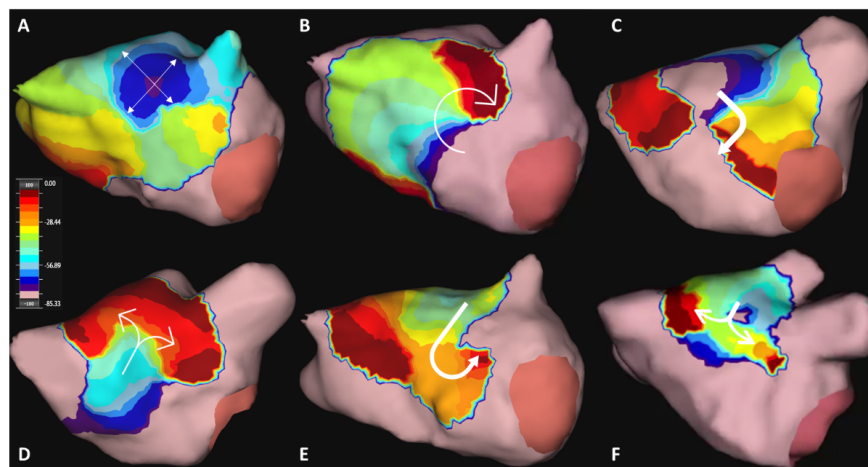across two repeated mapping segments of 30seconds duration.

	LIA	LIA	LRA	LRA	FF	FF	High frequency FF	High frequency FF
	LA	**RA**	**LA**	**RA**	**LA**	**RA**	**LA**	**RA**
R^2 value	0.81 (0.75-0.88)	0.84 (0.61-0.88)	0.39 (0.25-0.53)	0.41 (0.23-0.58)	0.58 (0.50-0.76)	0.66 (0.60-0.73)	0.80 (0.66-0.87)	0.83 (0.76-0.

Data are expressed as median (interquartile range).

Table 3 Cohen kappa statistic comparing the consistency of regions identified with the highest frequency of LIA, LRA and FF at the 30% cut off in both the LA and RA.

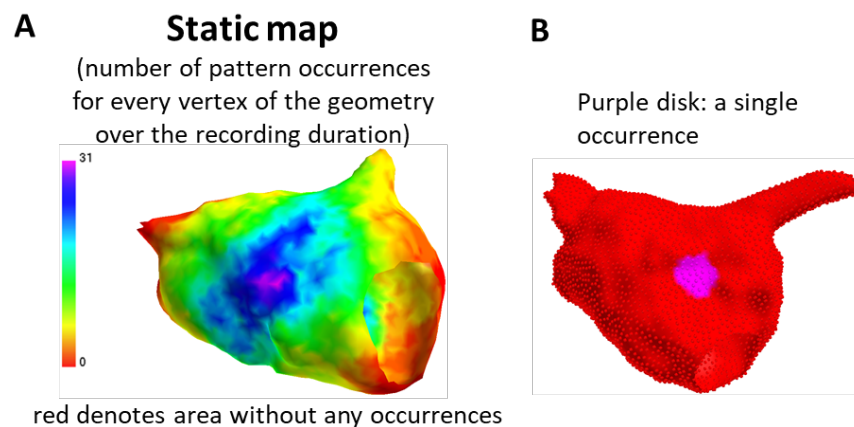|	LIA	LIA	LRA	LRA	FF	F
	LA	RA	LA	RA	LA	R
Median (interquartile range)	0.75 (0.64-0.78)	0.75 (0.58-0.79)	0.43 (0.33-0.49)	0.40 (0.28-0.47)	0.56 (0.47-0.64)	0.

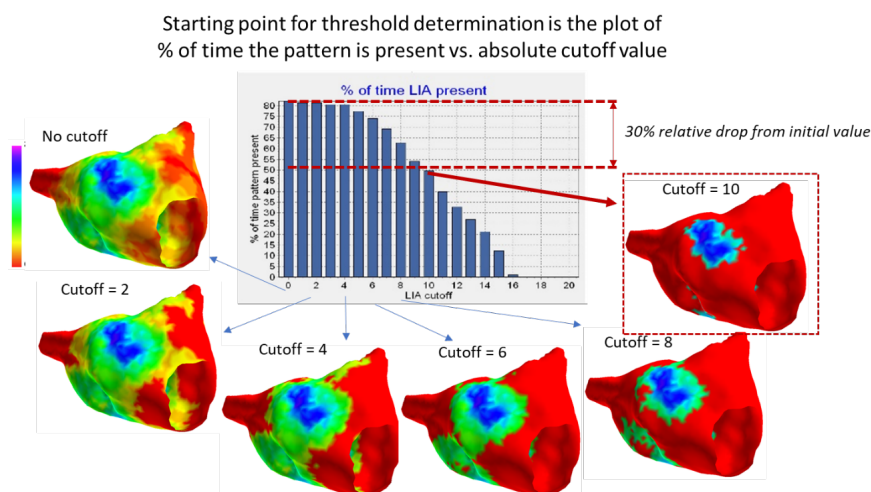Data are expressed as median (interquartile range).

Figure 1 Dynamic AcQTrack analysis assigns highlighted discs when each pattern is detected showing in pink for FF (A) characterised by radial activation from a central earliest point, green for LRA (B) where smooth rotational activation of >270° is observed; and yellow for LIA (C). LIA includes a range of specific patterns of activation, all characterised by changing wavefront direction of >90° (C-F, dynamic AcQTrack detection not shown). Colour scale depicts the leading (red) to trailing edge (purple) of a wavefront with the full colour spectrum occupying 80ms.
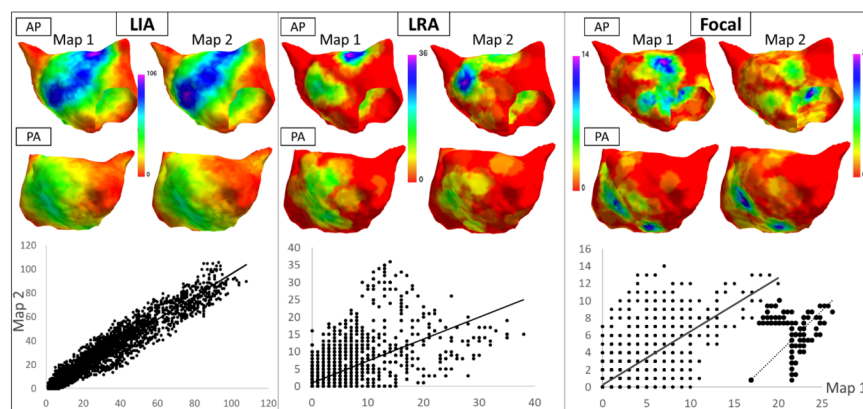

Figure 2 Fluoroscopic image of catheters positioned for simultaneous bi-atrial non-contact mapping.

12

A **Static map**

(number of pattern occurrences
for every vertex of the geometry
over the recording duration)

B

Purple disk: a single
occurrence

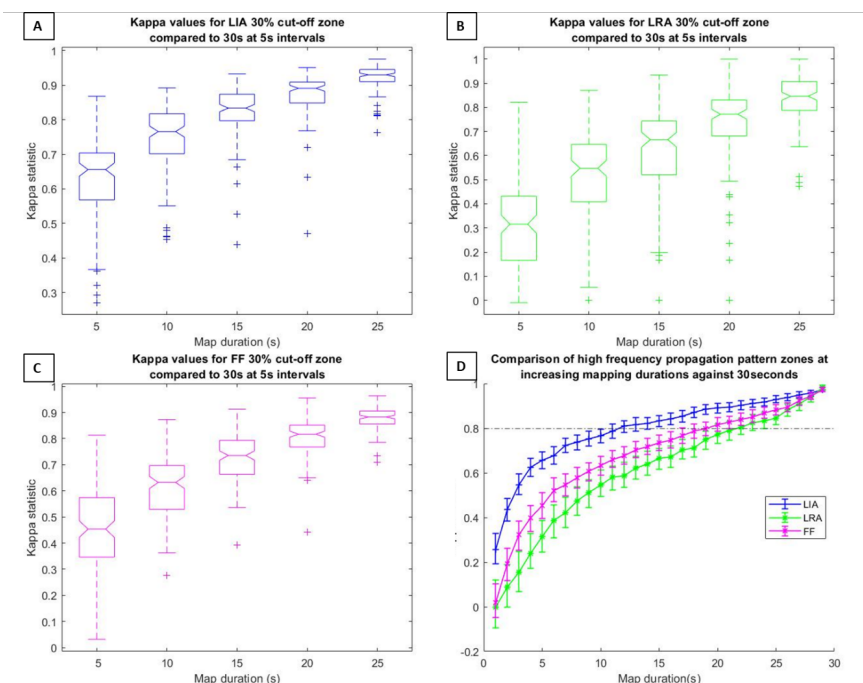red denotes area without any occurrences

Figure 3 Method for AcQTrack pattern quantification. A static map is generated (A) quantifying all pattern occurrences at every vertex of the chamber anatomy. Each occurrence is identified in space and time as a single disc allowing calculation of the total number of occurrences, the percentage time they are present, and the proportion of the chamber surface area affected. See also supplementary figure S3.

Figure 4 Threshold method. Cut off values for LIA are generated according to the total time the pattern is detected using thresholds gradually excluding more infrequent occurrences. (See text for detailed explanation)

13

Figure 5 Antero-posterior (top row) and postero-anterior (lower row) views the left atrium showing the density and distribution of localised irregular activation, localised rotational activation and focal firing (red=no occurrences, purple=highest density) in patient 10. Each pair of images represent 2 sequential 30s maps. Graphs below represent correlation plots for each anatomy vertex (1st map X axis, 2nd Y axis) with R^2 for LIA 0.92, LRA 0.39 and FF 0.49. Inset graph shows correlation for regions with FF frequency [?]1 every 3s on the first map with R^2 of 0.74.

Figure 6. Boxplots (A-C) showing the distribution of kappa values in 5-second increments for regions with high frequency (at the 30% cut off) LIA, LRA and FF respectively compared to the result after 30-seconds. Kappa values for the LIA, LRA and FF are shown at 1-second increments in (D) showing the point at which the kappa value (representing a very good level of agreement) reaches 0.8. LIA: Localised irregular activation, LRA: Localised rotational activation, FF: Focal firing.

Hosted file

14

Supplementary video `1_FF.mp4` available at https://authorea.com/users/403312/articles/514830-spatial-and-temporal-variability-of-rotational-focal-and-irregular-activity-practical-implications-for-mapping-of-atrial-fibrillation

Hosted file

Supplementary video `2_LRA.mp4` available at https://authorea.com/users/403312/articles/514830-spatial-and-temporal-variability-of-rotational-focal-and-irregular-activity-practical-implications-for-mapping-of-atrial-fibrillation

Hosted file

Supplementary video `3_LIA.mp4` available at https://authorea.com/users/403312/articles/514830-spatial-and-temporal-variability-of-rotational-focal-and-irregular-activity-practical-implications-for-mapping-of-atrial-fibrillation